

Perturbation theory for scalable solid-state quantum computation, and single-spin measurement using magnetic resonance force microscopy

Gennady Berman

Outline

1. Model: Ising spin chain for scalable quantum computation.
2. Perturbation approach (slow and fast dynamics; small parameters).
3. Examples: teleportation and quantum full adder.
4. MRFM single-spin measurement (CAI and OSCAR)



OUR TEAM

G.P. Berman (LANL, T-13)

F. Borgonovi (Brescia, Italy)

G.D. Doolen (LANL, T-13)

F. Izrailev (Puebla U., Mexico)

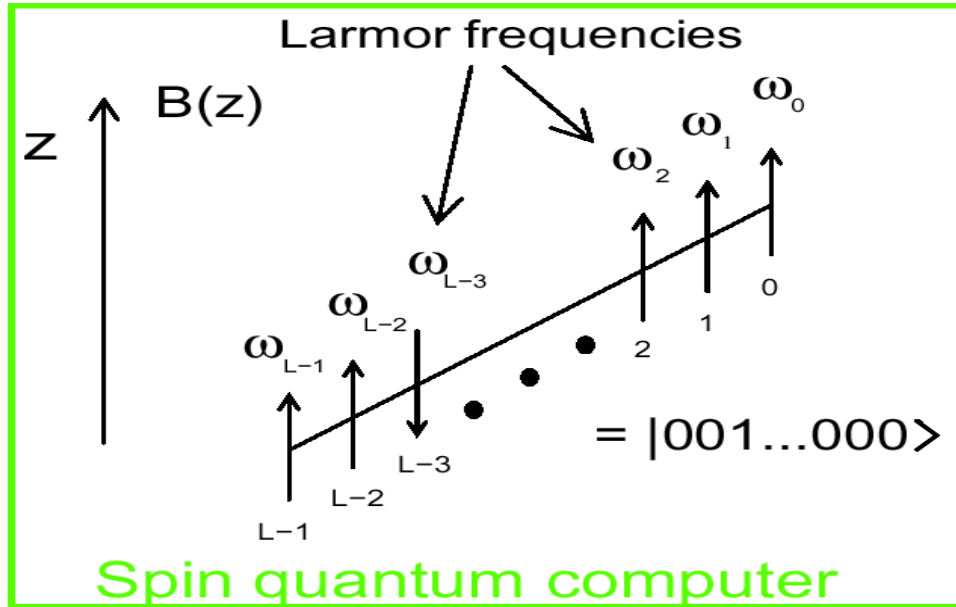
D.I. Kamenev (LANL, T-13/CNLS)

G.V. Lopez (U. de Guadalajara, Mexico)

R. Kassman (LANL, T-13/CNLS)

V.I. Tsifrinovich (NY Polytech. U.)

1000 qubit spin quantum computer

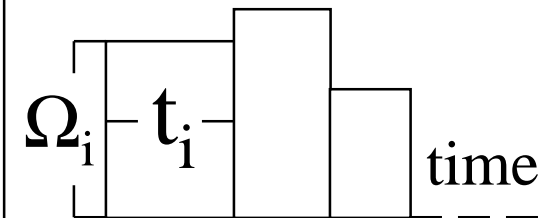


$T=0$

Pulses
 $\leftarrow b_i(t)$

$\uparrow - J - \uparrow$

Protocol:



Circular polarized magnetic field: $b_i(t) = b_i(\cos(\omega_i t + \phi_i), -\sin(\omega_i t + \phi_i), 0)$

$$\omega_k = \gamma B_z(z_k)$$

Number of qubits: L

Izing constant: J

Frequency difference:

$$\delta\omega = \omega_{k+1} - \omega_k$$

γ - gyromagnetic ratio

Rabi frequencies:

$$\Omega_i = \gamma b_i$$

Dynamics of a quantum computer

1. Quantum computer Hamiltonian:

$$H = - \sum_{k=0}^{L-1} \omega_k I_k^z - 2J \sum_{k=0}^{L-1} I_k^z I_{k+1}^z + V(t), \quad \text{pulses: } V(t) = \sum_{n=1}^M V_n(t),$$

$$V_n(t) = -\frac{\Omega_n}{2} \sum_{k=0}^{L-1} \left\{ I_k^- \exp[-i(\omega_n t + \phi_n)] + I_k^+ \exp[i(\omega_n t + \phi_n)] \right\},$$

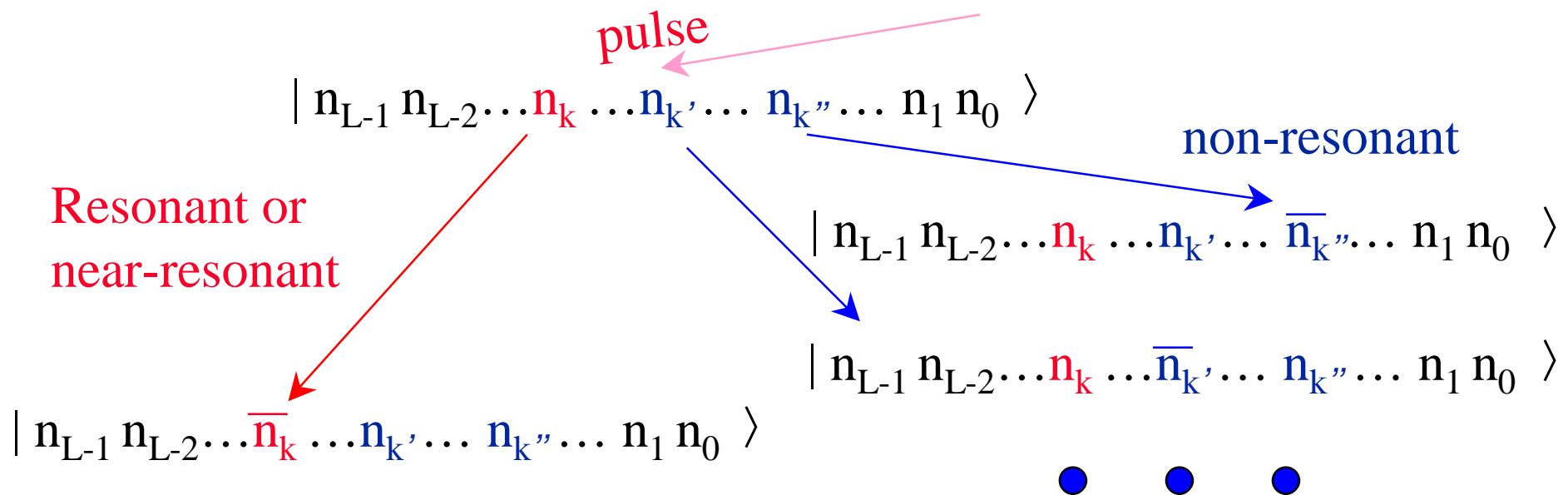
I_k^z is the z-component of k th spin,

$$I_k^+ = I_k^x + iI_k^y, \quad I_k^- = I_k^x - iI_k^y,$$

2. **Strategy:** in order to remove time-dependence in H we:

- (a) make transformation to the frame rotating with the frequency ω_n ,
- (b) use eigenstates of the effective Hamiltonian to compute transition probabilities.

Resonant (slow) and non-resonant (fast) dynamics



n_k and \overline{n}_k indicate the spins with opposite orientation

Pulse which is resonant for a given qubit acts also on all other qubits producing many **unwanted** states with small probabilities.

Perturbation theory based on diagonalization of large sparse matrices

Eigenstates of the **Hamiltonian** \longrightarrow Evolution operator

Structure of Hamiltonian sparse matrix 2^{L-1} of 2×2 blocks and connections (one-spin-flip non-resonant transitions) between them:

$$\left(\begin{array}{cc|cc|cc|cc|cc} E_m & V & V & 0 & 0 & 0 & V & 0 & \cdot & \cdot \\ V & E_p & 0 & V & 0 & 0 & 0 & V & \cdot & \cdot \\ \hline V & 0 & E_{m'} & V & V & 0 & 0 & 0 & \cdot & \cdot \\ 0 & V & V & E_{p'} & 0 & V & 0 & 0 & \cdot & \cdot \\ \hline 0 & 0 & V & 0 & E_{m''} & V & 0 & 0 & \cdot & \cdot \\ 0 & 0 & 0 & V & V & E_{p''} & 0 & 0 & \cdot & \cdot \\ \hline V & 0 & 0 & 0 & 0 & 0 & E_{m'''} & V & \cdot & \cdot \\ 0 & V & 0 & 0 & 0 & 0 & V & E_{p'''} & \cdot & \cdot \\ \hline \cdot & \cdot & \cdot & \cdot & \cdot & \cdot & \cdot & \cdot & \cdot & \cdot \\ \cdot & \cdot & \cdot & \cdot & \cdot & \cdot & \cdot & \cdot & \cdot & \cdot \end{array} \right)$$

Matrix Size:
 $2^L \times 2^L$

Interaction between blocks:
 $V = -\frac{\Omega}{2}$

$$|E_p - E_m| \propto J \text{ or } |E_p - E_m| = 0, \quad |E_p - E_{p'}| \propto \delta\omega, \quad |V| \ll J \ll \delta\omega$$

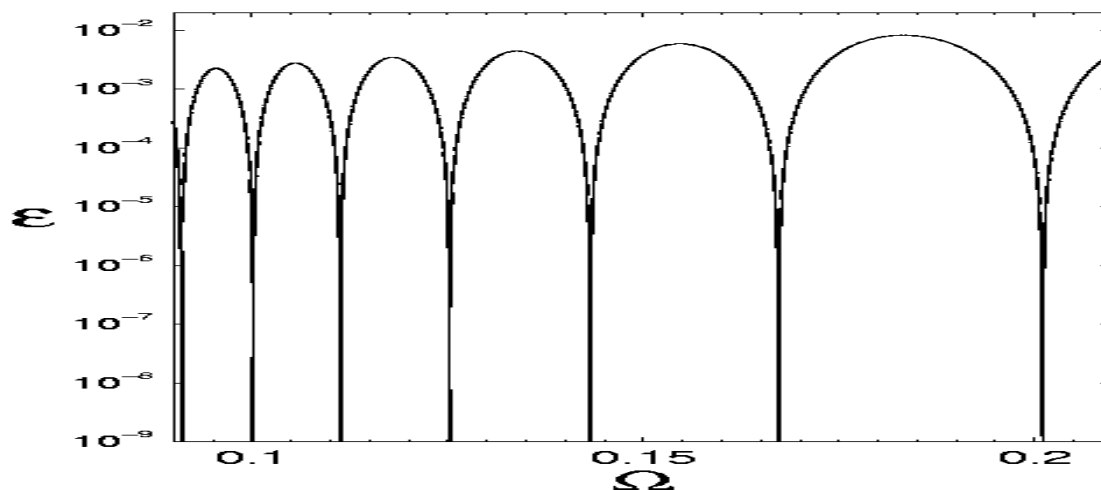
Small parameters

Perturbation theory: $\Omega \ll J \ll \delta\omega$

Probability of **near-resonant** transitions

$$\varepsilon = \left[\frac{\Omega}{\lambda} \sin(\lambda\tau) \right]^2$$

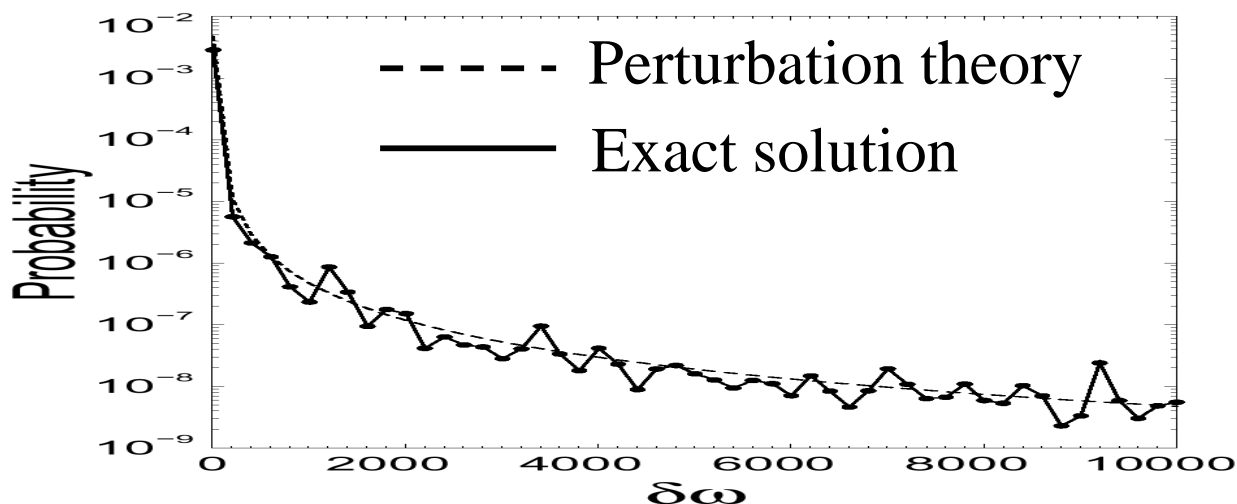
$$\lambda^2 = \Omega^2 + 4J^2$$



Probability of **non-resonant** transitions ($\varepsilon = 0$)

$$\mu \approx \left(\frac{\Omega}{\delta\omega} \right)^2 f(L)$$

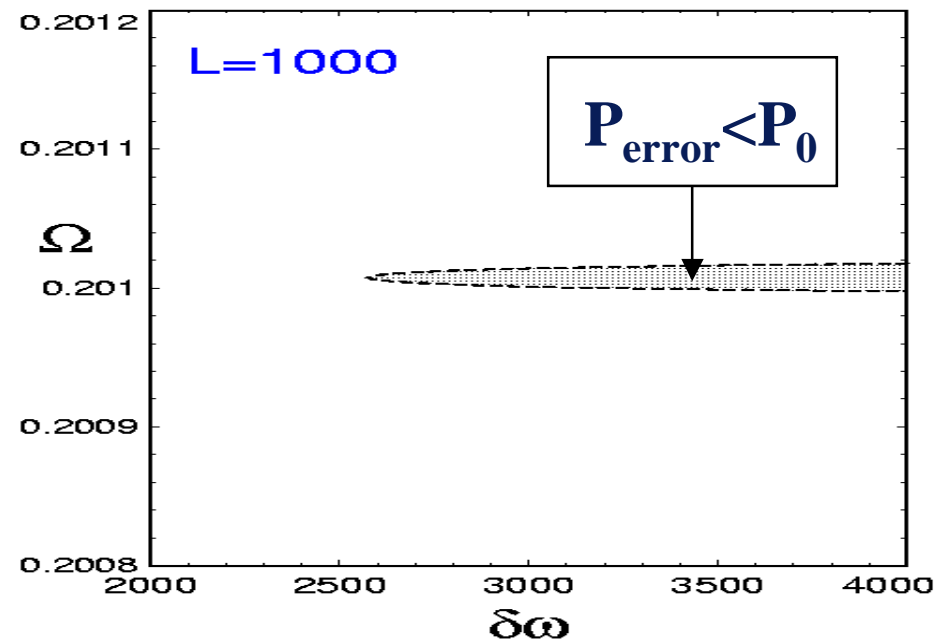
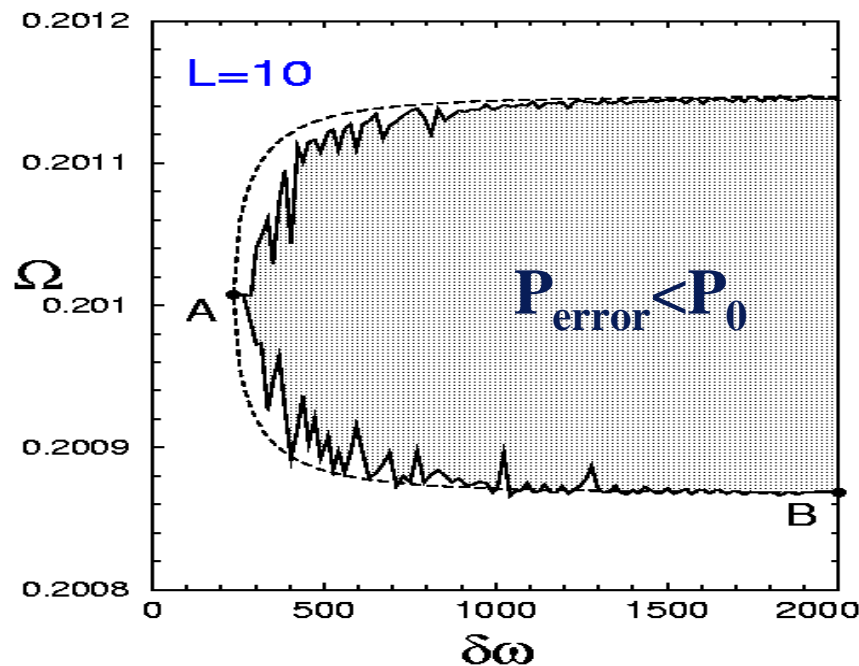
$$f(L) \approx 2L - 2$$



Numerical results for error-controlled quantum computation

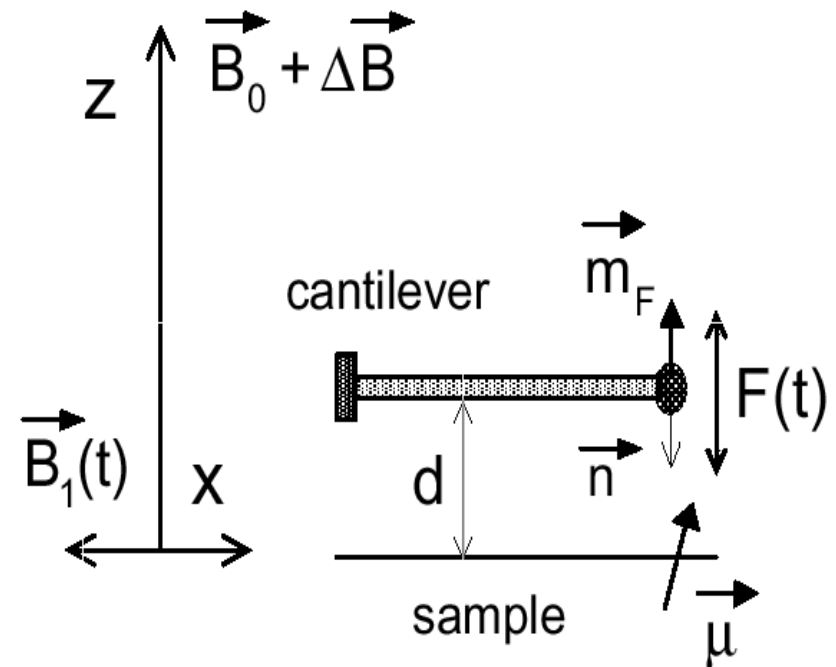
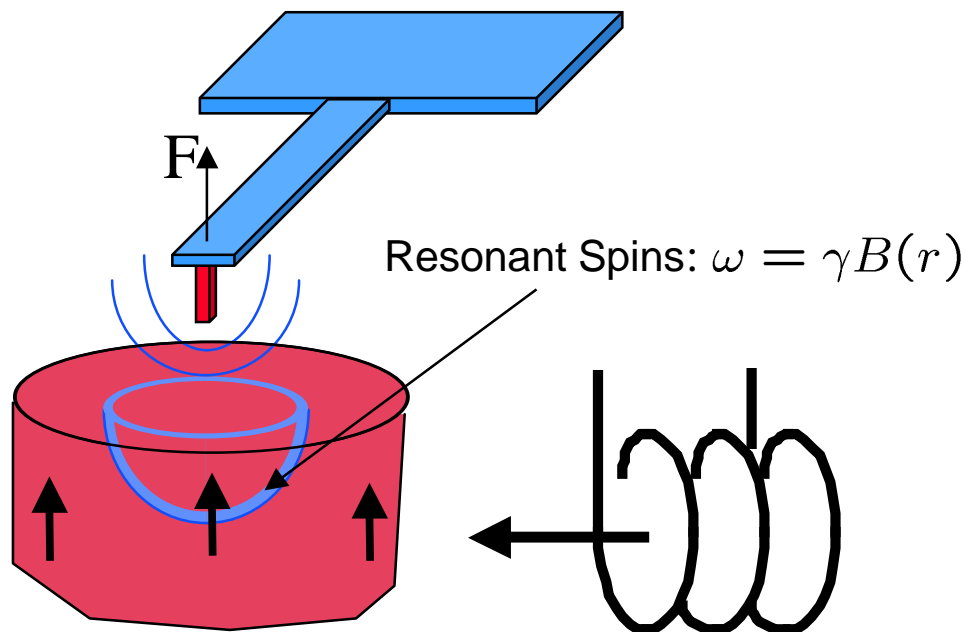
The total probability of error computed using the perturbation theory for small and for large number of qubits. Inside the hatched regions the probability is less than $P_0=10^{-5}$.

— improved perturbation theory
 - - - perturbation theory



MRFM single spin resolution

Simulations of MRFM cyclic adiabatic inversion (CAI) with phase modulation



$$\vec{B}_1(t) = B_1^0 \{ \cos[\omega t + \phi(t)], -\sin[\omega t + \phi(t)] \}$$

Signal-to-noise ratio (classical approach)

Amplitude of driven oscillations

$$Z_c \approx -i \frac{QF}{k_c} e^{i\omega_c t}$$

quality factor Q force $F = \gamma \eta \nabla B_z / 2$ spring constant k_c

Amplitude of thermal noise

$$Z_{rms} = \sqrt{\frac{4Qk_B T \Delta f}{k_c \omega_c}}$$

bandwidth Δf temperature T

Requirement for detection: $|Z_c / Z_{rms}| > 1$

For the ultrathin cantilever [T.D.Stowe *et al.*, Appl. Phys. Lett. **71**, 288 (1997)], $\Delta f = 0.4$ Hz, $\omega_c / 2\pi = 1.7$ kHz, $Q = 6700$, $k_c = 6.5 \times 10^{-6}$ N/m:

$$\frac{\partial B}{\partial z} > 9 \times 10^4 \sqrt{T}$$

The Hamiltonian for MRFM with CAI

$$\mathcal{H} = \underbrace{\frac{P_z^2}{2m_c^*} + \frac{m_c^* \omega_c^2 Z^2}{2}}_{\text{Harmonic oscillator}} - \underbrace{\hbar \left(\omega_L - \omega - \frac{d\varphi}{dt} \right) S_z}_{\text{Zeeman Interaction}} - \underbrace{\hbar \omega_1 S_x}_{\text{Excitation}} - \underbrace{g\mu \frac{\partial B_z}{\partial Z} Z S_z}_{\text{Spin-Cantilever Coupling}} + \underbrace{H_e + H_{ce} + H_{se}}_{\text{Environment}}$$

H_e – the Hamiltonian of environment

H_{ce} – the Hamiltonian of cantilever-environment interaction

H_{se} – the Hamiltonian of spin-environment interaction

Effective magnetic field

$$\vec{B}_{eff}(t) = \frac{1}{\gamma_e} \left(\omega_1, 0, \omega_L - \omega - \frac{d\varphi}{dt}(t) + \gamma_e Z \frac{\partial B_z}{\partial Z} \right)$$

Nonlinear interaction important in OSCAR
when frequency shift is measured

Classical limit: classical cantilever and classical spin magnetization

Parameters from: *Rugar et al., Science, 264,1560 (1994)*

- *Two interaction parameters*

force exerted by spin on cantilever

$$\eta = \frac{g\mu(\partial B_z / \partial Z)}{2\sqrt{k_c}\eta\omega_c}$$

quantum force

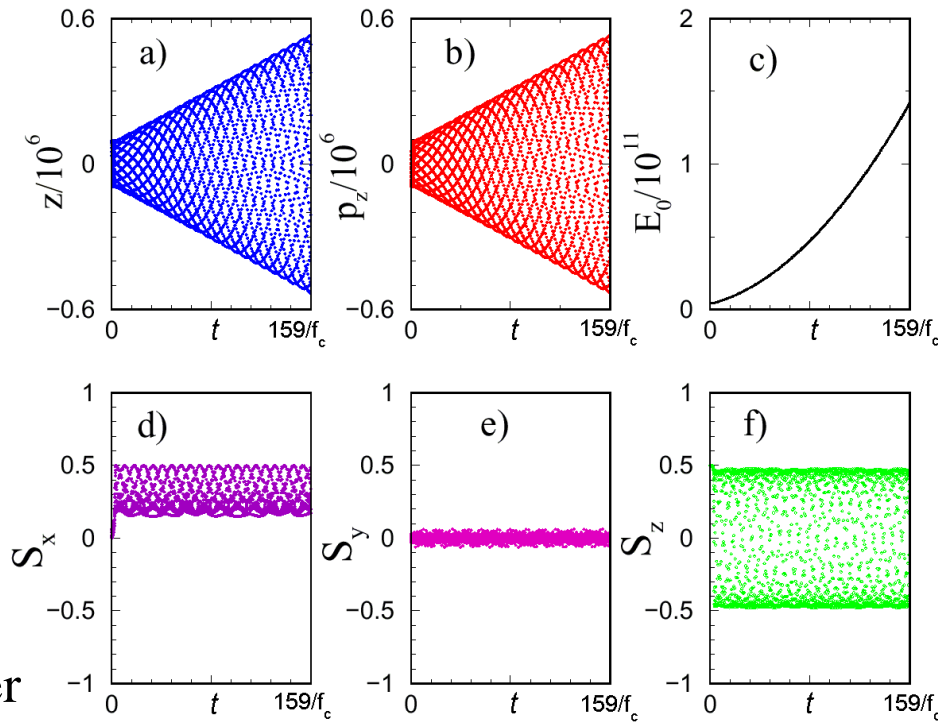
$$\varepsilon = \frac{\gamma B_1^0}{\omega_c}$$

← Rabi frequency

← frequency of cantilever

$\eta = 2.8 \times 10^{-7}$ ← is extremely small in *Rugar et al.*

$\eta \sim 10^{-3}$ ← for single spin



Schrödinger equation for evolution of wave function

$$i\eta \frac{\partial \Psi(z,t)}{\partial t} = \hat{H} \Psi(z,t)$$

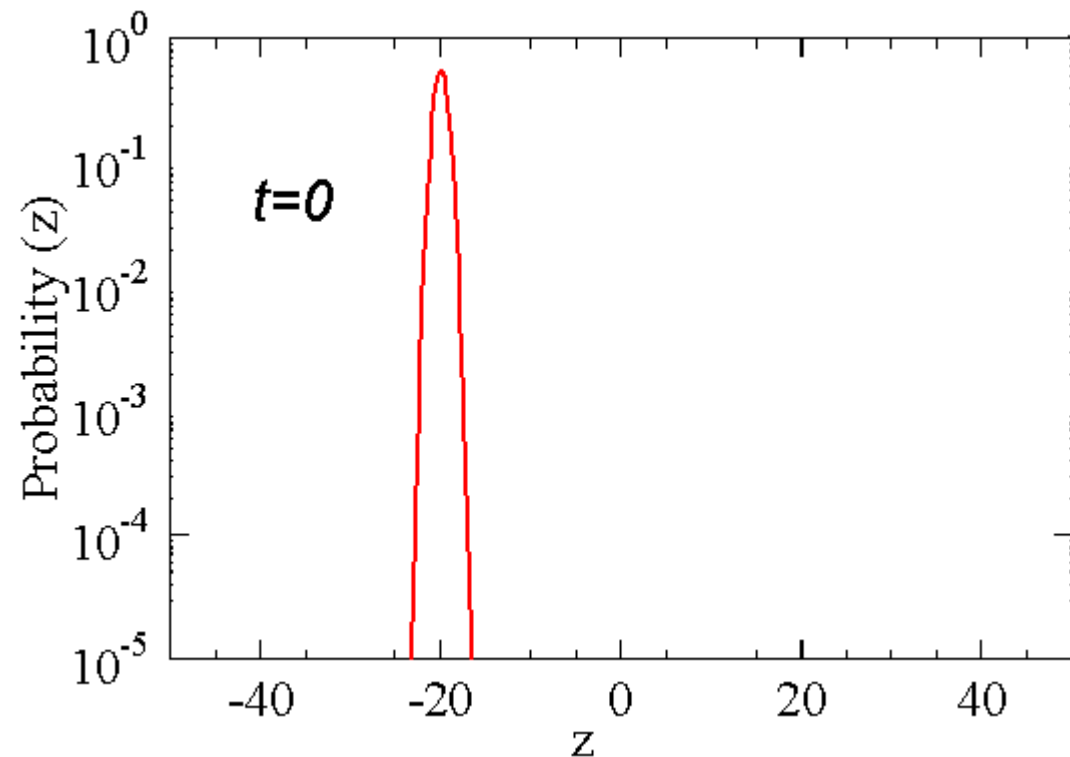
$$\Psi(z,t) = \Psi_1(z,t) |\uparrow\rangle + \Psi_2(z,t) |\downarrow\rangle$$

- *Cantilever is prepared in a “quasi-classical” state*

$$\eta = 0.3$$

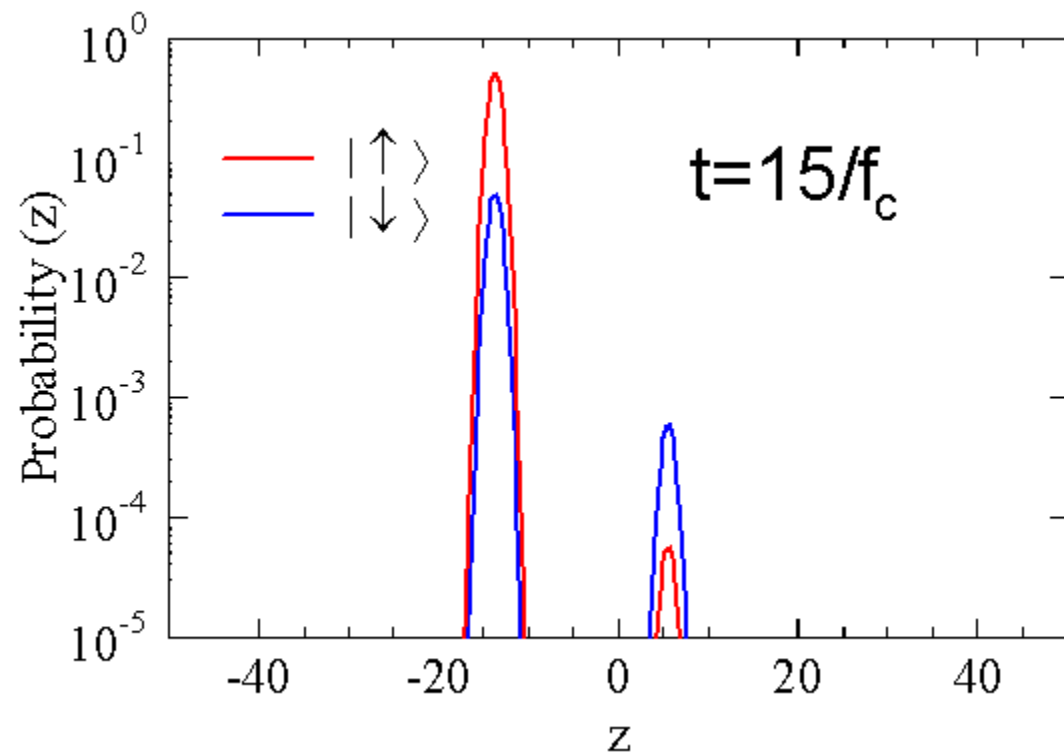
$$\varepsilon = 400$$

$$z = Z / \sqrt{\eta \omega_c / k_c}$$

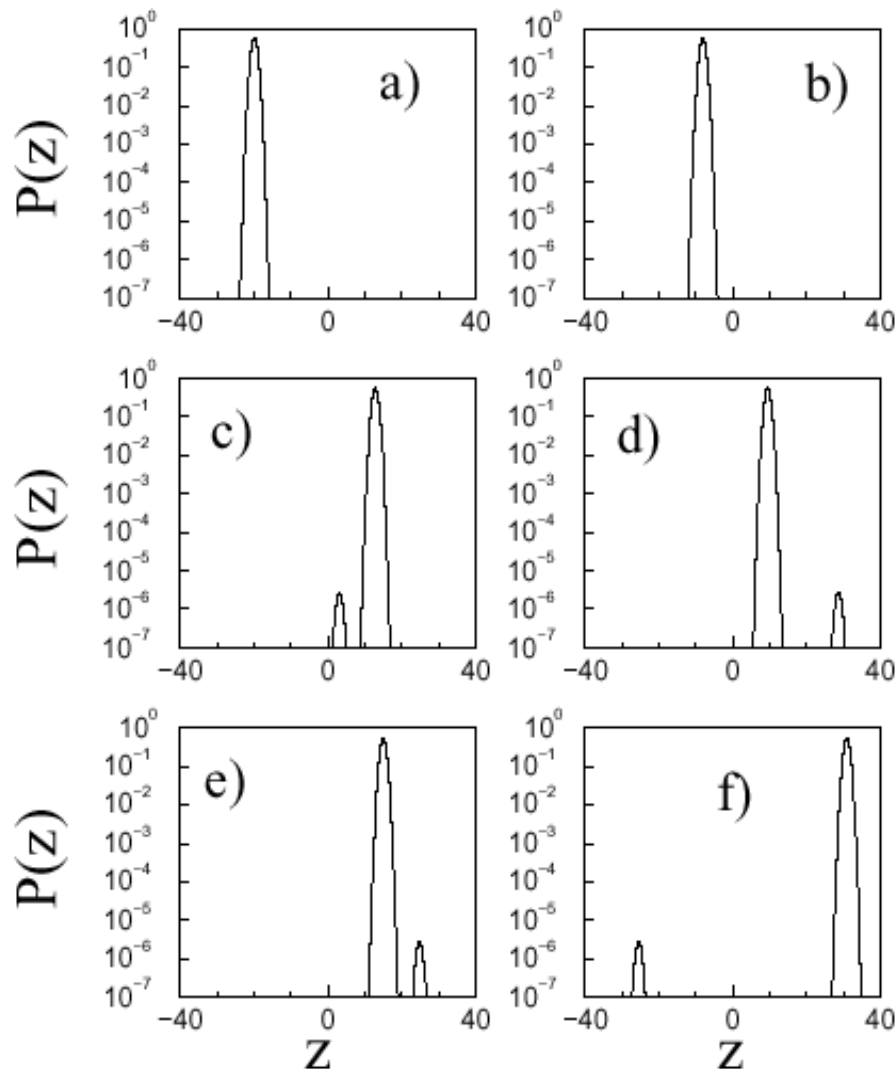


Schrödinger cat state for the cantilever

- *Cantilever is prepared in a “quasi-classical” state*
- *Asymmetric “Schrödinger cat” cantilever state develops due to coupling to spin*
- *Two heads of the cantilever are composed of both spin states*



Probability distribution of the cantilever coordinate for different times



Two heads of the cat oscillate periodically in time!

Probability distribution of the cantilever coordinate z for $\varepsilon=400$ and $\eta=0.3$. The initial conditions: $z(0) = \langle z \rangle = -20$, $p_z(0) = \langle p_z \rangle = 0$, and the average spin is in the direction of the effective magnetic field.

Orientation of the average spin in each head of the Schrödinger cat

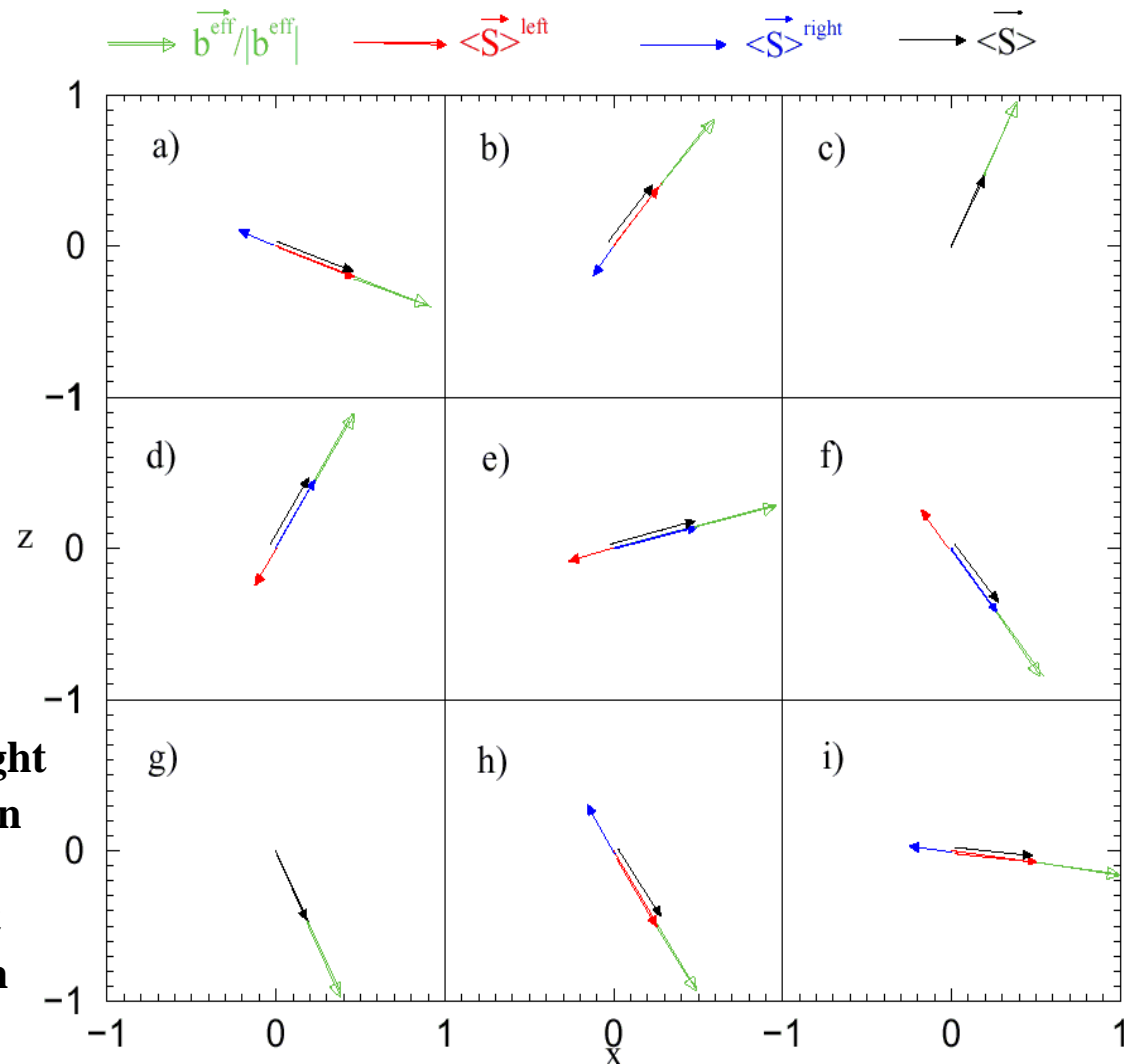
- Total wave function is **entangled**

$$\Psi \neq \Psi_{\text{cantilever}} \otimes \Psi_{\text{spin}}$$

- Wave functions in each head are **disentangled!**

$$\Psi^{\text{right}} = \Psi_{\text{cantilever}}^{\text{right}} \otimes \Psi_{\text{spin}}^{\text{right}}$$

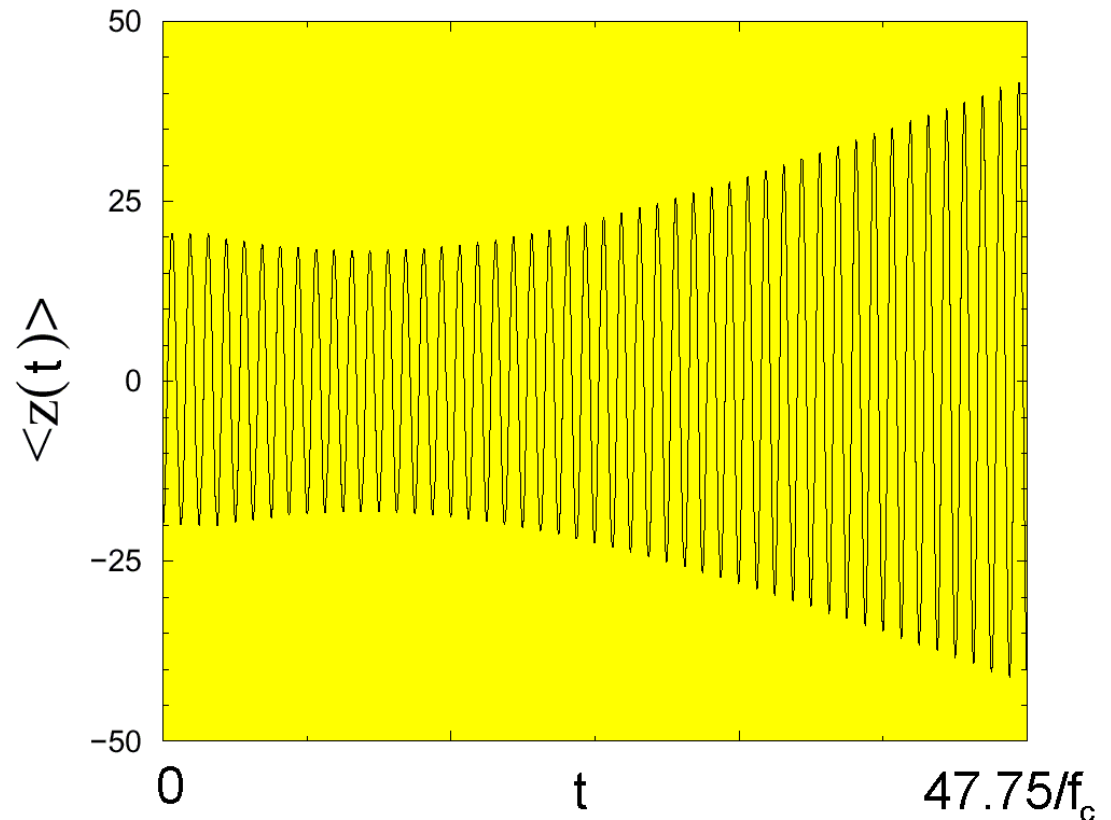
$$\Psi^{\text{left}} = \Psi_{\text{cantilever}}^{\text{left}} \otimes \Psi_{\text{spin}}^{\text{left}}$$



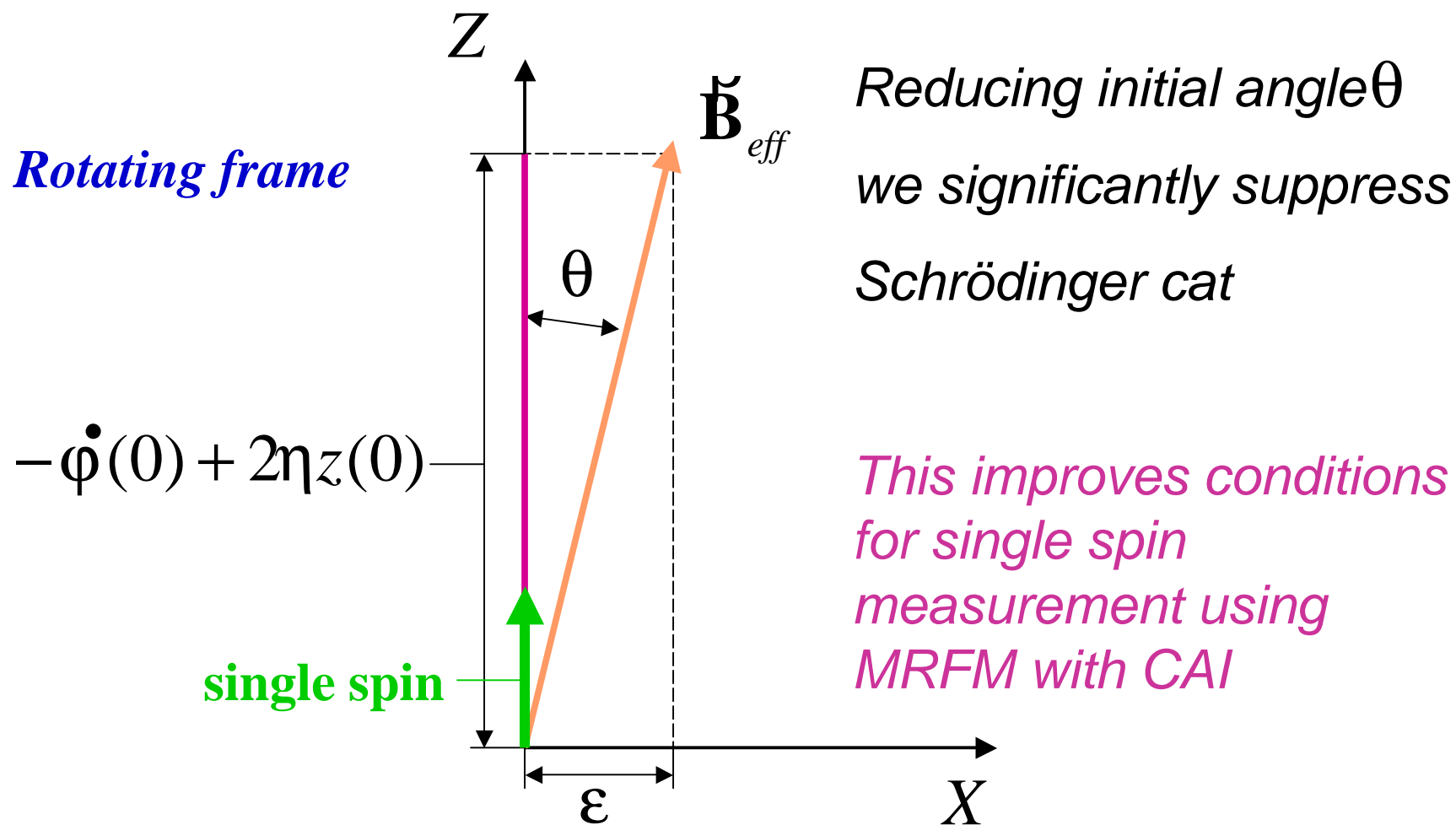
Average amplitude of the cantilever

$$\langle Z(t) \rangle = \langle \Psi(z, t) | Z | \Psi(z, t) \rangle$$

- *Although the “Schrödinger cat” appears, on average the cantilever is excited*



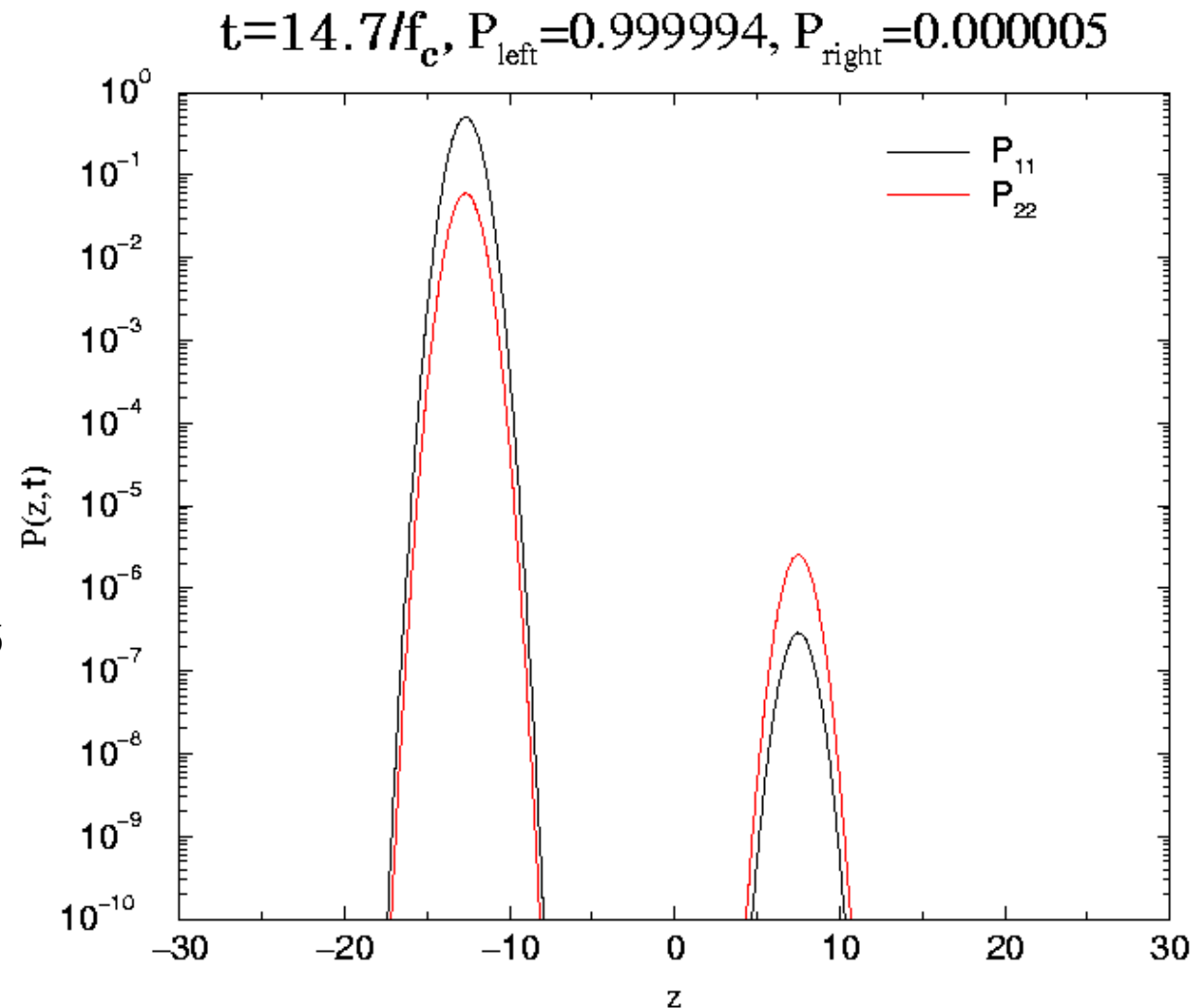
Suppression of Schrödinger cat state in MRFM with CAI



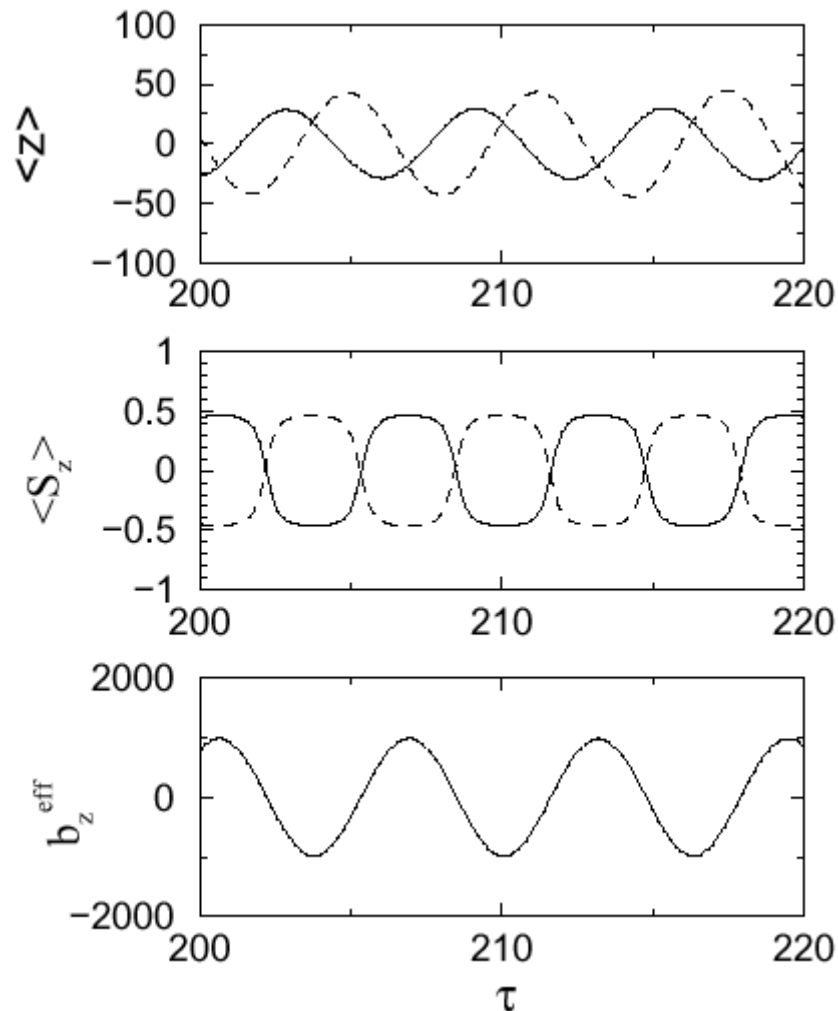
Suppression of Schrödinger cat state in MRFM with CAI

At $t=0$ spin is oriented approximately in the direction of $\vec{\mathbf{B}}_{eff}$

Probability of small head is $5 \cdot 10^{-6}$



Measurement of spin state in MRFM with CAI using a cantilever phase



Measurement of the single-spin state using the phase of the cantilever vibrations. For the dynamics of $\langle z(\tau) \rangle$ and $\langle S_z(\tau) \rangle$ the solid line corresponds to “big” (classical) peak of the SC state, and the dashed line corresponds to “small” (quantum) peak of the SC state renormalized to the similar amplitudes. At the bottom the dynamics of the z -component of the effective field is shown.

Finite-temperature approach to MRFM with CAI

$$\mathcal{H} = \underbrace{\frac{P_z^2}{2m_c^*} + \frac{m_c^* \omega_c^2 Z^2}{2}}_{\text{Harmonic oscillator}} - \underbrace{\hbar \left(\omega_L - \omega - \frac{d\varphi}{dt} \right) S_z}_{\text{Zeeman Interaction}} - \underbrace{\hbar \omega_1 S_x}_{\text{Excitation}} - \underbrace{g\mu \frac{\partial B_z}{\partial Z} Z S_z}_{\text{Spin-Cantilever Coupling}} + \underbrace{H_e + H_{ce} + H_{se}}_{\text{Environment}}$$

We are calculating a reduced density matrix equation for this Hamiltonian and finding the dependences of the dynamics of spin detection in MRFM CAI with phase modulation and in OSCAR, on:

1. Quality factor of the cantilever, Q
2. Diffusion coefficient, D
3. The interaction force with magnetic particle, η
4. The amplitude of the *rf* field, ε .

Decoherence time for the cantilever

(G.P. Berman *et al.*, PRA **61**, 032311 2002)

$$\frac{t_d}{t_c} \approx \frac{\omega_c}{k_c k_B T} \left(\frac{\eta}{Z_{rms}} \right)^2 = \left(\frac{\eta \omega_c}{2k_B T} \right)^2 \frac{\omega_c}{Q_c \Delta f}$$

$t_c = Q_c / \omega_c$ – time-constant of the cantilever

$Z_{rms} = \sqrt{\frac{4Qk_B T \Delta f}{k_c \omega_c}}$ – the amplitude of the thermo-mechanical noise

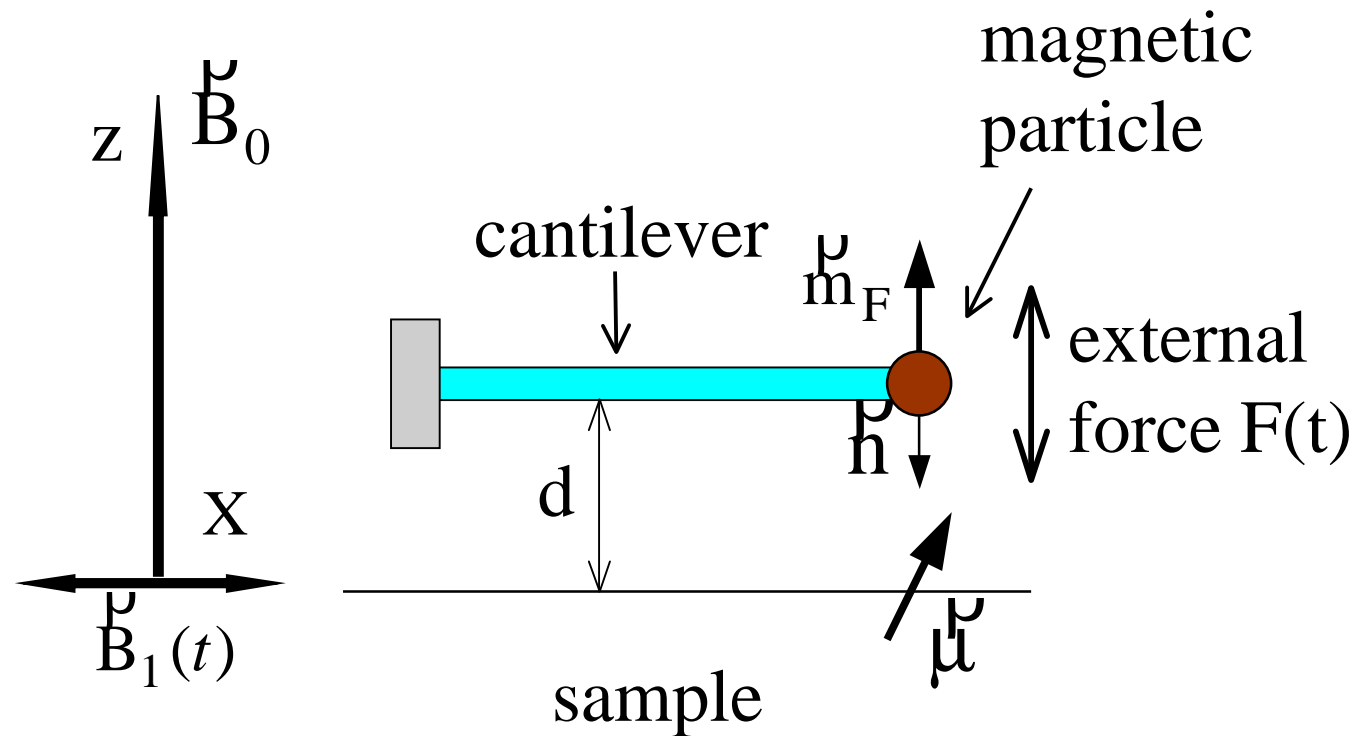
For an ultrathin cantilever [T.D.Stowe *et al.*, Appl. Phys. Lett. **71**, 288 (1997)], $\Delta f = 0.4$ Hz, $\omega_c / 2\pi = 1.7$ kHz, $Q = 6700$, $k_c = 6.5 \times 10^{-6}$ N/m,

the decoherence time is extremely small

$$t_d / t_c \approx 7 \times 10^{-15} / T^2 \quad (t_c = Q_c / \omega_c \approx 0.6 \text{ s})$$

Spin quickly jumps in (or opposite) the direction of the effective magnetic field

Dynamical modeling of MRFM – OSCAR technique



Method for measuring the frequency shift of the cantilever

Nonlinear oscillations of the **cantilever** are described by the equation:

$$\ddot{z} = f(z, \dot{z}, t, \mu),$$

where f is the nonlinear function of z .

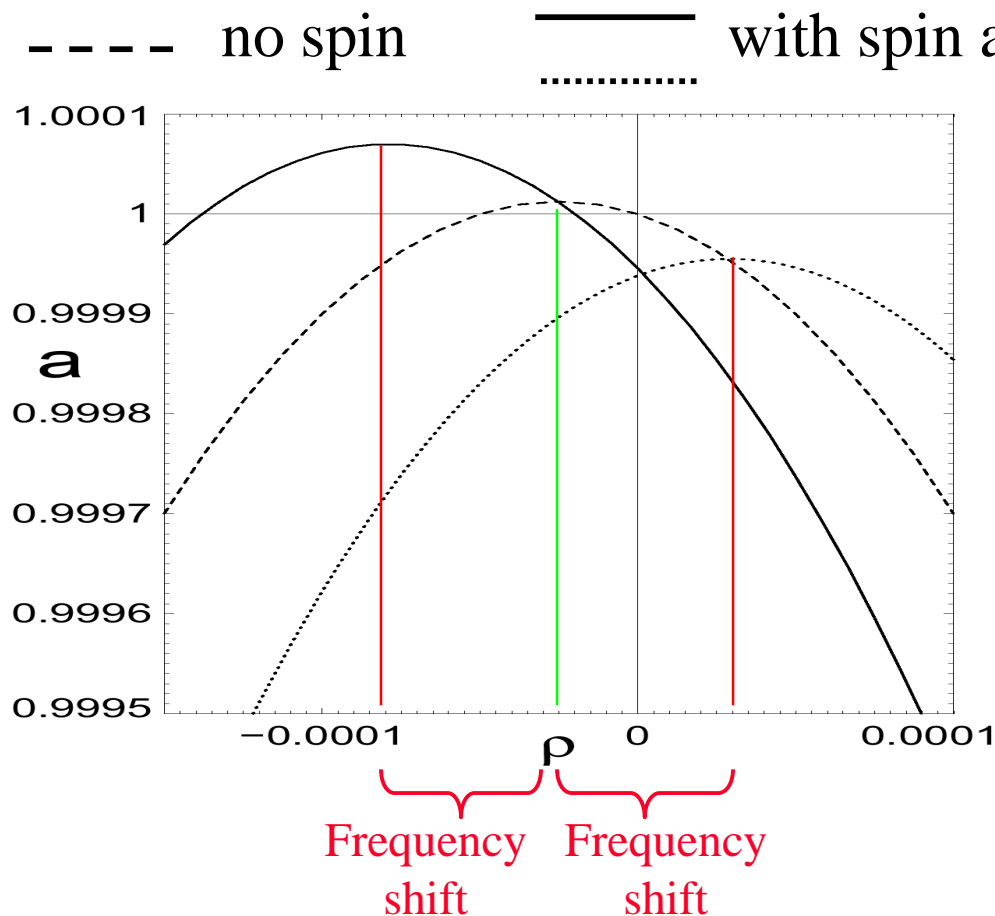
Dynamics of the **spin** is given by the equation:

$$\dot{\mu} = g(z, \mu)$$

The influence of the **spin** on the dynamics of the **cantilever** results in the frequency shift of the **cantilever**.

The frequency shift of the cantilever in OSCAR technique

Dependence of the amplitude a of the driven oscillations of the cantilever on the detuning ρ . The values a and ρ are dimensionless. The value $a=1$ is the amplitude of driven oscillations of the cantilever in the case of exact resonance, when $\nu=\omega_c$ ($\rho=0$) without spin.



$$\rho = (\nu - \omega_c) / \omega_c$$

ν - frequency of external mechanical force acting on the cantilever

ω_c - frequency of small oscillations of the cantilever

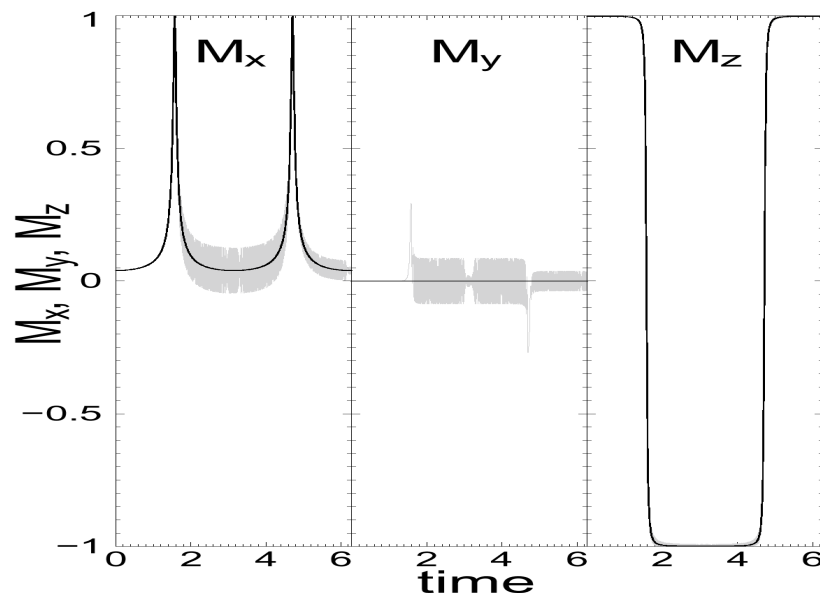
For reasonable parameters and for $\omega_c/2\pi = 10^5$ Hz the **frequency shift** per one magneton is ≈ 6 Hz.

Cyclic adiabatic inversion conditions in OSCAR technique

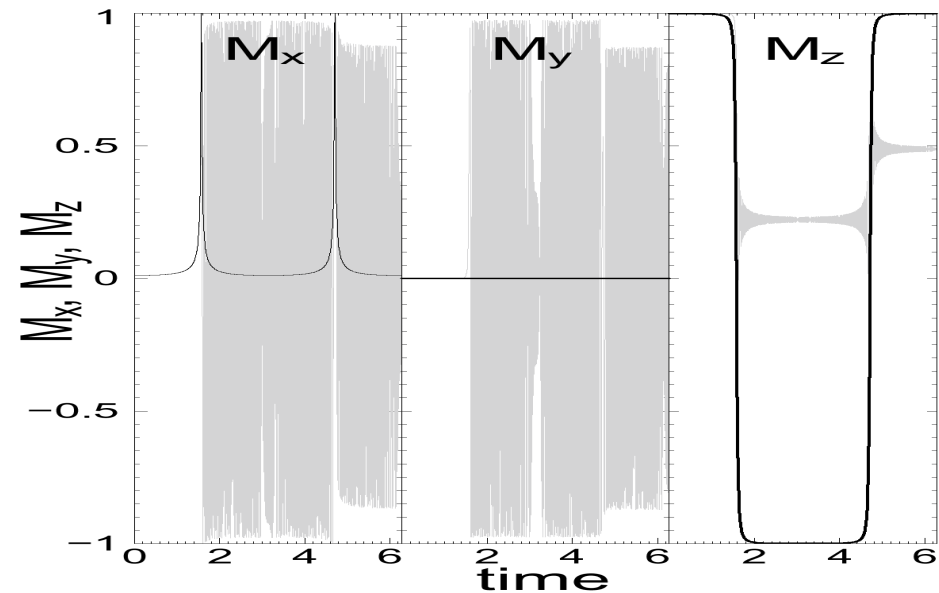
In order to make the influence of the spin on the cantilever strong enough the average dynamics of the spin should be coherent with the dynamics of the cantilever. To provide this, the amplitude of the time-dependent magnetic field, B_{\perp} , must be large, $\varepsilon = \gamma B_{\perp} / \omega_c \gg 1$, where γ is the gyromagnetic ratio. M_x , M_y , and M_z are the components of the spin measured in units of Bohr magneton.

- - Numerical simulations
- - Analytic solution for averaged dynamics

$\varepsilon=280$



$\varepsilon=28$



Dynamical theory of MRFM- OSCAR with many spins

We use discrete equations for magnetic moments in the resonant slice

$$\dot{\boldsymbol{\mu}}_k = -\gamma \boldsymbol{\mu}_k \times \mathbf{B}_{eff,k} \quad - \text{ magnetic moment in the } k\text{th cube}$$

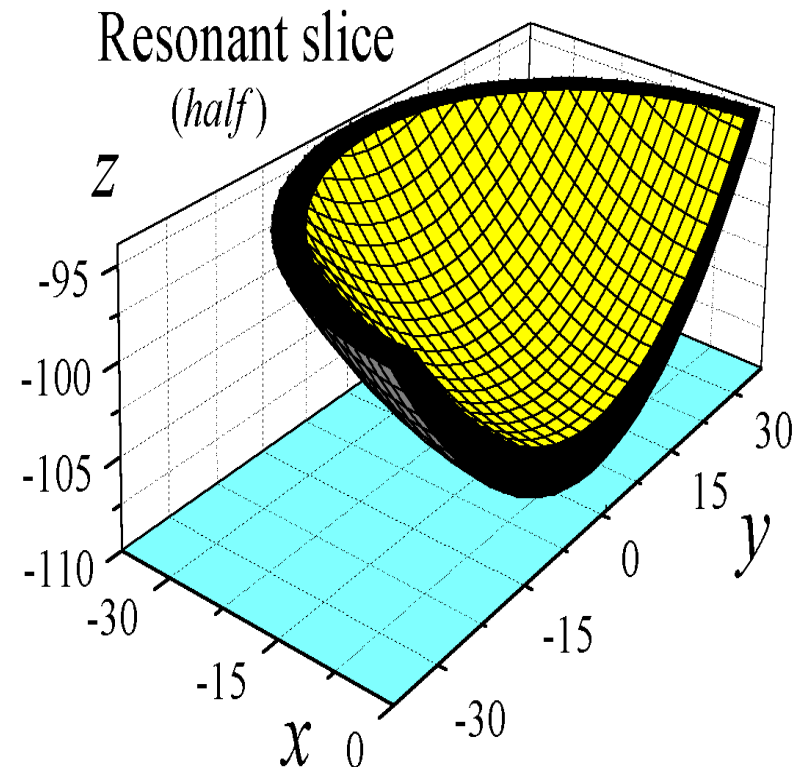
$$\mathbf{B}_{eff,k} = \mathbf{B}_{ext} + \frac{\mu_0}{4\pi} \frac{3(\mathbf{m} \cdot \mathbf{h}_k) \mathbf{h}_k - \mathbf{m}}{r_k^3}$$

\mathbf{m} - magnetic moment of the tip

$$\mathbf{r}_k = \mathbf{r}_k(z_c)$$

The force acting on the cantilever:

$$\mathbf{F} = -\sum_k (\boldsymbol{\mu}_k \cdot \nabla) \mathbf{B}_{eff,k}$$



Recent publications

1. G. P. Berman, G. D. Doolen, G. V. Lopez, V. I. Tsifrinovich, A quantum full adder for a scalable nuclear spin quantum computer, *Computer Physics Communications*, **146**, 324 (2002).
2. G. P. Berman, D. I. Kamenev, and V. I. Tsifrinovich, Perturbation theory for quantum computation with a large number of qubits, *Phys. Rev. A* **65**, 032311 (2002).
3. G. P. Berman, G. D. Doolen, P. C. Hammel, and V. I. Tsifrinovich, Static Stern-Gerlach effect in magnetic-force microscopy, *Phys. Rev. A* **65**, 032311 (2002).
4. G. P. Berman, D. I. Kamenev, and V. I. Tsifrinovich, Stationary Cantilever vibrations in oscillating-cantilever-driven adiabatic reversals: Magnetic-resonance-force-microscopy technique, *Phys. Rev. A* **66**, 023405 (2002).
5. G. P. Berman, F. Borgonovi, G. Chapline, P. C. Hammel, and V. I. Tsifrinovich, Magnetic-resonance force microscopy measurement of entangled spin states, *Phys. Rev. A* **66**, 032106 (2002).
6. G. P. Berman, F. Borgonovi, G. V. Lopez, V. I. Tsifrinovich, Transient dynamics in magnetic force microscopy for a single-spin measurement, quant-ph/0210006.